Polish J. Chem., **78**, 1907–1924 (2004)

Quantum Chemical Modelling of the Oxidation of Myoglobin

by E. Ilkowska[1], M. Witko[2*], R. Tokarz-Sobieraj[2] and G. Stochel[1]

[1]*Faculty of Chemistry, Jagiellonian University, ul. Ingardena 3, 30-060 Cracow, Poland*
fax: +48 12 636 53 92; e-mail: stochel@chemia.uj.edu.pl
[2]*Institute of Catalysis and Surface Chemistry, Polish Academy of Sciences,*
ul. Niezapominajek 8, 30-239 Cracow, Poland
fax: +48 12 425 19 23; e-mail: ncwitko@cyf-kr.edu.pl

(Received February 9th, 2004; revised manuscript April 29th, 2004)

The electronic structure (charge distribution, bond indices) and the geometry (bond distances and angles) of the deoxyheme and the oxyheme with coordinated proximal histidine in their reduced and oxidized form were determined by the INDO method. The effect of the distal histidine (in the case of the oxyheme) and a water molecule (in the case of the metheme) on the geometry, charge distribution and stability of the systems was investigated. The method was adopted to model the oxidation of myoglobin in biological systems. The results revealed that both deoxy- and oxymyoglobin could spontaneously undergo one-electron oxidation. The mechanistic considerations based on the charge distribution and energetic effects led to the conclusion, that in oxymyoglobin's case the electron transfer are followed by dissociation of a dioxygen molecule and addition of a water molecule, where both processes proceed in parallel.

Key words: oxyheme, deoxyheme, electronic structure, oxidation process, ZINDO method

Although biological reactions involving heme-proteins have been extensively examined by many research groups [1–4], there is still a lot of questions, which need to be answered. One of the recently studied phenomena concerns the role of oxygen carrying hemoproteins, such as hemoglobin (Hb) and myoglobin (Mb) in the intracellular redox processes. It has been found, that both these proteins can reduce metal ions in aerobic conditions of the cell [5,6]. *In vitro* studies on model systems, consisting of Hb or Mb and Cu(II) or Fe(III) complexes, have been performed by spectroscopic, kinetic and other experimental methods [5–16]. The reduction potential, the stability constant, and the nature of the electron transfer orbitals of the metal-chelate are found to influence the rate and the mechanism of metal chelates reduction. Generally, two mechanisms of reduction of Fe(III) and Cu(II) chelates by hemoglobin or myoglobin are suggested. The first is a simple outer-sphere mechanism, in which an electron transfer occurs over the heme edge, and the second one is a site- specific mechanism, requiring the formation of a metal-chelate-protein ternary complex prior to the elec-

*Author for correspondence.

tron transfer. It is assumed, that in both mechanisms the only redox active species are the deoxy globins [5,6].

On the basis of the results obtained by conventional kinetic methods for the reduction of the hexacyanoferrate(III) by the myoglobin both an inner-sphere electron transfer [10] and an outer-sphere [11] electron transfer with deoxyMb (Mb), as the only redox reactive species, according to Scheme 1, are postulated.

$$MbO_2 \rightleftharpoons Mb + O_2 \qquad Mb + Fe(CN)_6^{3-} \longrightarrow \text{met-Mb} + Fe(CN)_6^{4-} \tag{1}$$

Our conventional and high-pressure kinetic studies, as well as structural and electrostatic modelling, performed for the reduction of pentacyanoferrates(III) ($[Fe(CN)_5L]^{n-}$, where $L = CN^-, NO_2^-, H_2O$) by myoglobin indicate, that the outer-sphere mechanism is operating and both oxy- and deoxymyoglobin are redox active species (Scheme 2) [12,16].

$$\begin{array}{ccc} & \overset{K_1}{\rightleftharpoons} & \\ Mb + O_2 & & MbO_2 \\ + Fe(CN)_5L^{n-} \downarrow & & \downarrow + Fe(CN)_5L^{n-} \\ \text{met-Mb} + Fe(CN)_5L^{(n+1)-} & & \text{met-Mb} + Fe(CN)_5L^{(n+1)-} + O_2 \end{array} \tag{2}$$

As the starting point to discuss, the reactivity of any hemeprotein, its geometry as well as the electronic structure of the heme moiety has to be considered. The X-ray structures of myoglobin are determined for its three forms: deoxymyoglobin (Mb) [17], oxymyoglobin (MbO_2) [18], and metmyoglobin (met-Mb) [19]. Myoglobin is a monomer with a polypeptide chain of 153 amino acids. This globin is attached to the oxygen-binding prosthetic group (iron(II) with protoporphyrin IX) by coordination to the iron through the imidiazole ring of a proximal histidine residue. Deoxymyoglobin (Mb) has a pentacoordinated iron(II) centre, in which the metal atom lies 0.42 Å out of the plane, formed by the four pyrrole-rings and binds to the donor nitrogen atoms. It is displaced towards the bound imidazole group, *i.e*. the proximal side of the heme. Upon binding of dioxygen, (O_2), which yields oxymyoglobin (MbO_2), the iron atom moves toward the FeN_4 plane. The dioxygen molecule is bound end-on to the iron centre, forming a bent structure with a Fe–O–O bond angle equal to 115°. Although the properties of oxygen binding to the natural proteins as hemoglobin and myoglobin are extensively studied, the nature of the iron–oxygen bond in these molecules is still a controversial issue. Generally to describe the Fe-O_2 bonding two models are used: Pauling's model (Fe^{2+}-O_2) [20] and Weiss' model (Fe^{3+}-O_2^-) [21].

The whole spectrum of experimental techniques, like Moessbauer spectroscopy, electronic spectroscopy, magnetic circular dichroism, infrared spectroscopy, Raman spectroscopy, and magnetic susceptibility are used to elucidate the bonding of oxygen to iron porphyrins and hemoproteins [1,4]. In parallel, many theoretical calculations [22–30] are performed to resolve uncertainties and to account for the observed properties of oxyhemoglobin and oxymyoglobin. A qualitative *ab initio* Hartree-Fock study of the structure of the metalloproteins requires excellent computational facilities, as model systems involve many atoms. In addition, the results of the *ab initio* studies, performed for various oxyheme models do not give one definite description of the Fe-O_2 bonding. The type of the model, as well as the quality of the used basis set have a strong influence on the electronic structure of the heme-moiety and, as a consequence, the obtained wavefunctions consisted mostly of various percentages of the two suggested configurations: the Fe^{2+}-O_2, with the closed-shell state $^1A'$ [23,25,26], and the Fe^{3+}-O_2^- with the open-shell state $^3A'$ [27].

Previous semiempirical [28] and DFT [29] approaches, used to study the oxyheme models, have focused mainly on the charge distribution within the porphyrin complex induced by the geometry changes. It was found, that a decrease in the iron-oxygen distance slightly favours the charge transfer from the iron to O_2 molecule. On the other hand, the increasing O–O distance enhances the negative charge on the dioxygen. Moreover, the bent end-on structure of the Fe-O_2 bond caused an excess of a negative charge, which may be easily accommodated on the terminal oxygen atom. The hydrogen bond between O_2 molecule and the protein polypeptide chain also favours the bent end-on Fe-O_2 conformation.

In this paper, we model the one-electron oxidation of myoglobin in oxy- and deoxy form by the semiempirical ZINDO method. The goal is to understand the mechanism of the biological intracellular oxidation of myoglobin or hemoglobin under aerobic conditions by combining the results obtained both from the present theoretical approach and the previous kinetic experiments. As the first step the geometric, as well as electronic structures of all redox forms of the model compounds are optimized. Then, on the basis of the geometrical, electronic and energetic results the possible reaction pathways are discussed.

MODELS AND METHODS

The electronic and geometric structures are obtained by the ZINDO method [31–36], which has been proved to be suitable to interpret the behaviour of biological systems [37–43]. The details of the method, which gives, as any other semiempirical treatment, only the qualitative picture, are described elsewhere (see, for example [37–43] and references therein). Here, we give only a quick overview of this method. The ZINDO method is characterized by the inclusion of all one-centre exchange terms, necessary for rotation invariance and accurate spectroscopic predictions. The method uses a basis set of Slater-type orbitals (STO), which are then envisioned as being symmetrically orthogonalized to one another. A basis set of single Slater-type orbitals (STO) is characterized by the choice of exponential constants. For hydrogen the value of 1.2 is taken, whereas for elements of the second and third rows the exponents derived from Slater's rules are used [35]. One-centre core integrals are calculated from the ionization potentials.

One-centre resonance integrals are set to zero, whereas the two-centre one-electron integrals are calculated. The nuclear attraction integrals are proportional to two-centre Coulomb integrals between the appropriate atoms. The two-electron two-centred nonvanishing integrals are evaluated over STO's, similarly to the one-centre integrals.

The optimization of geometry is performed by Newton-Raphson and Hessian methods [36]. Vacuum calculations are carried out and no influence of a reaction field is taken into account. The electronic structures are analysed using atomic Mulliken populations [44] and Mayer bond orders [45–46]. Atomic charge distribution provides the information about the charging of atoms, forming the system and about the ionic (electrostatic) contribution to the binding in the system. The bond order analysis may serve as a measure of the bond strength and allows the estimation of the covalent contribution to the total bond.

A pentacoordinated iron with the porphyrine IX ring and the proximal histidine group as the fifth ligand modeles the myoglobin active centre. In the case of oxymyoglobin, the sixth ligand, *i.e*. a dioxygen molecule is added (Figure 1). As a starting point for the geometry optimization, the experimental geometry [18] is assumed for both species.

Despite the fact, that pentacyanoferrate(III) complexes are used in our kinetic experiments as the acceptor of an electron in the oxidation of myoglobin, in theoretical model we do not include those complexes. Here, the redox process is modelled by decreasing the number of electrons in the heme systems. The geometry optimization is done for the all redox forms collected in Table 1. In the next step the model with a distal histidine, added to the oxyheme system is investigated (Figure 2), to check the influence of this residue on the geometric and electronic properties of the oxyheme.

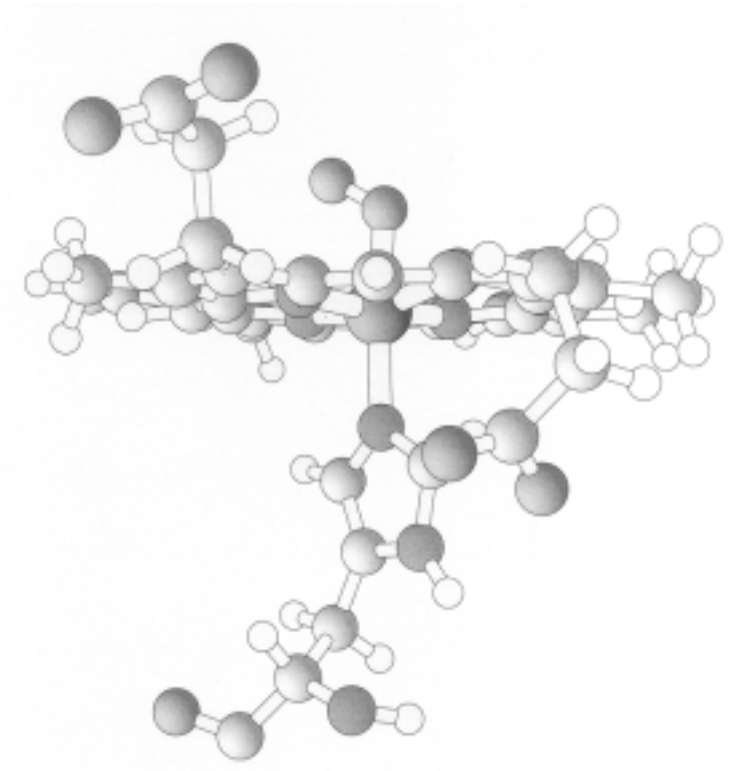

Figure 1. Geometrical structure of the oxyheme with coordinated proximal histidine residue obtained by the ZINDO method.

Table 1. Studied systems.

Model	Symbol	Number of the valence electrons
Deoxyheme	heme	272
Oxidized deoxyheme	$heme^+$	271
Oxyheme	$hemeO_2$	284
Oxidized oxyheme	$hemeO_2^+$	283
Aqua-metheme	metheme–H_2O	279

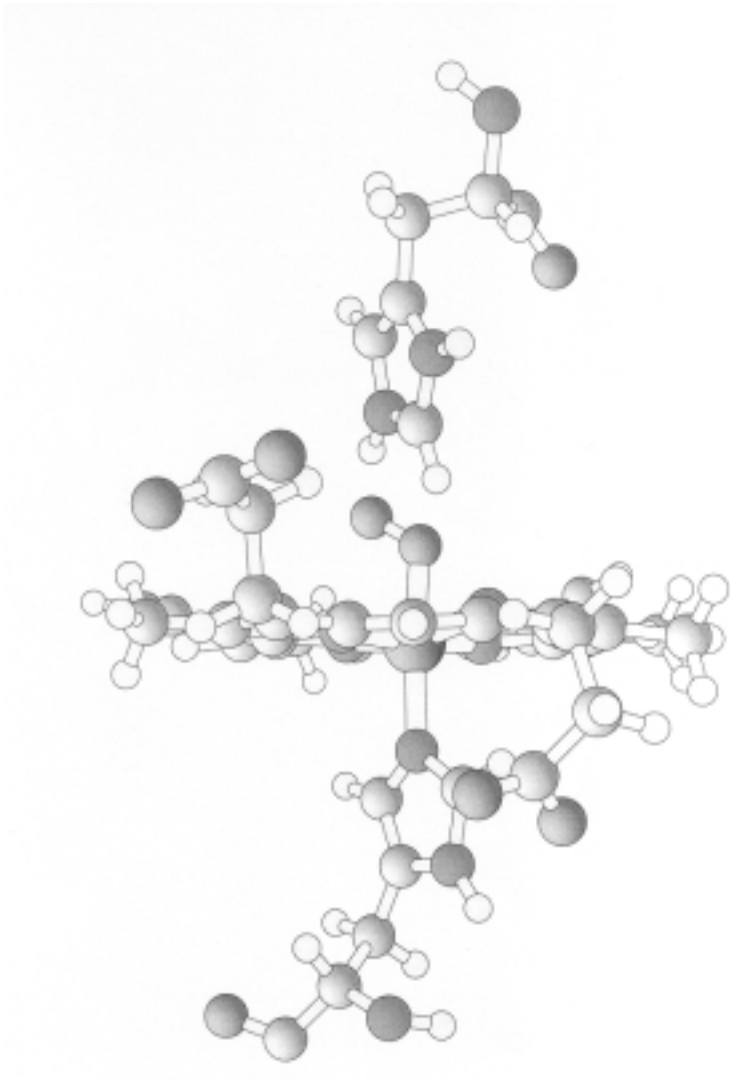

Figure 2. Geometrical structure of the oxyheme with proximal and distal histidine residues obtained by the ZINDO method.

During the geometry optimization procedure, the porphyrin ring is kept frozen, while the proximal histidine residue, the iron atom and both oxygen atoms are allowed to rearrange. The reaction pathway for the oxidation process is discussed.

RESULTS AND DISCUSSION

In large biological systems, like myoglobin or even heme alone, there is a spectrum of molecular orbitals, which have similar energies, and it is difficult to judge univocally the electronic configuration of the ground state for these systems. Therefore, in our calculations all possible multiplicities for the studied system are taken into account and geometry optimizations are performed separately for each of them.

Deoxyheme system: Theoretically the deoxyheme can exist in three electronic states, which differ in multiplicity (*i.e.* 1, 3 and 5, corresponding to 0, 2 and 4 unpaired electrons localised on the Fe atom). Table 2 summarizes the total energies of the system, as well as the electronic parameters, such as charges on Fe, N of proximal histidine (his_p), charges on the selected fragments of the molecule, as well as bond orders for those states.

Table 2. Relative energies (0 value refers to the multiplicity with the lowest energy) and selected electronic properties for the different electronic states of the deoxyheme (heme) system.

	singlet	triplet	quintet
Energy [kJ/mol]	154.90	110.27	0
Charges on atom or molecular fragments			
Fe	0.78 ($s^{0.356}p^{0.645}d^{6.224}$)	0.76 ($s^{0.365}p^{0.645}d^{6.234}$)	0.76 ($s^{0.411}p^{0.703}d^{6.131}$)
N(his)	–0.21	–0.21	–0.22
proximal histidine	–0.31	–0.30	–0.26
porphyrin ring	–2.47	–2.46	–2.50
Bond order Fe–N(his)	0.27	0.27	0.38

The total energy of the system depends on the state multiplicity and decreases with increasing the number of unpaired electrons. The energy obtained for the quintet state is significantly lower than the energy for the singlet and the triplet. The energy difference between the singlet and the triplet states is equal to 44.63 [kJ/mol], whereas between the triplet and the quintet states is twice as large and equals 110.27 [kJ/mol]. The theoretical results fully agree with experiment, claiming the high spin state for the deoxymyoglobin molecule [1,19].

The atomic charges (Fe, N(his_p)), which determine an ionic contribution to a chemical bond, do not depend on the multiplicity. Their values, different from the formal charges of Fe^{2+} and N^{3-}, suggest that the Fe–N(his_p) bond is a mixture of a covalent and ionic character. The bond order between Fe and N(his_p) depends on the multiplicity and is the largest one for the quintet state. This confirms the covalent contribution to that bond. The partial charge on the proximal histidine depends on the multiplicity, but not on the porphyrin ring.

The optimization procedure leads to a substantial movement of the Fe atom under the porphyrine plane and strongly depends on the spin state of the system. In the quintet state, the change of the iron position with reference to the porphyrin plane amounts to 0.4 Å, whereas for the singlet and triplet states is by 0.15 Å smaller. This result agrees with the experimental data, which indicates that the iron displacement is 0.42 Å [4,18].

Oxidized deoxyheme system: A similar treatment is repeated for the oxidized deoxyheme ($heme^+$), where the oxidation process is modelled by removing one electron from the system. For $heme^+$ three possible multiplicities are taken into account, *i.e.* 2, 4 and 6 (corresponding to 1, 3 and 5 unpaired electrons on the iron atom). The total energies and electronic properties (similar as for the deoxyheme) are collected in Table 3.

Table 3. Relative energies (0 value refers to the multiplicity with the lowest energy) and selected electronic properties for the different electronic states of the oxidized deoxyheme ($heme^+$) system.

	doublet	quartet	sextet
Energy [kJ/mol]	207.41	0	81.39
Charges on atom or molecular fragments			
Fe	0.76 ($s^{0.350}p^{0.666}d^{6.275}$)	0.76 ($s^{0.362}p^{0.648}d^{6.225}$)	0.73 ($s^{0.413}p^{0.716}d^{6.141}$)
N(his)	–0.22	–0.22	–0.21
proximal histidine	0.10	–0.25	0.11
porphyrin ring	–1.86	–1.51	–1.84
Bond order Fe–N(his)	0.35	0.32	0.23

Here, the energy of the system depends also on the multiplicity, but in contrast to the deoxyheme, the stability of the system does not simply increase with increasing the number of unpaired electrons. The quartet state is obtained as the ground state. The total energy of the sextet is 81.39 [kJ/mol] higher than of the quartet state, whereas the doublet seems to be the least stable state. In this case the energy difference is 207.41 [kJ/mol].

The analysis of the atomic charges on the Fe and N(his_p) shows, that they are similar for all states except for the sextet. In that case a small decrease of the positive charge on the iron and of negative on the nitrogen is observed. The atomic charges on the

Fe and N in all spin states point out a small ionic contribution and a clearly covalent character of these bonds. The bond order depends on the multiplicity and decreases with increasing the number of unpaired electrons. The state of the highest multiplicity is characterized by the weakest bond between Fe and proximal histidine. A reverse dependence is observed for the deoxyheme. Also partial charges on the proximal histidine and the porphyrin ring depend on the multiplicity of the system. While those values are similar for the doublet and the sextet states, they remarkably differ for the quartet state (by about 0.3 e). In this case, the negative charge is moved form the porphyrin ring into the proximal histidine.

As it was mentioned previously, the oxidized form of deoxyheme ($heme^+$) is a hypothetical system. Assuming the energy minimum criterion and taking into account the electronic properties of the different states, one can say that the results of calculations point out the quartet state as the ground one for the deoxyheme system.

Oxyheme system: The electronic structure of oxymyoglobin is a subject of many studies [22–28,47–51] and usually two structures are used for describing the bond between iron ion and dioxygen:

– Pauling's structure [20], where Fe^{2+} bounds to the neutral dioxygen molecule, Fe^{2+}-O_2 and
– Weiss' structure [21], in which Fe^{3+} is bound to the O_2^- ion as Fe^{3+}-O_2^-.

The oxyheme (*i.e.* heme with the dioxygen ligand coordinated to the iron centre in its sixth coordination site) is considered in order to model the active centre of oxymyoglobin. The possible electronic state for this system may correspond to one of the four different spin states (2S+1) = 1, 3, 5 and 7.

Table 4 contains the calculated total energies, as well as electronic properties for all the studied states. Similarly as it was in the case of the deoxyheme, the total energy depends on the multiplicity of the system and decreases with increasing the number of unpaired electrons. The most favourable, from the energy point of view, is the state of the highest multiplicity, while the singlet state, which corresponds approximately to Pauling's model, is the least stable one. Its energy is 215.55 kJ/mol higher than of the other states. The energy difference between the triplet (corresponding approximately to Weiss' model) and the quintet states amounts to 22 kJ/mol, whereas between the quintet and the heptet state to 46.73 kJ/mol. Singlet and triplet states can be realized in many different ways, which means that they are more probable than the other two states (quintet and heptet). Since in addition the experimental results suggest, that oxymyoglobin is a low spin species, the triplet state is assumed as the ground state for the oxyheme.

The net charge, localized on the iron atom for the singlet and triplet states, is almost the same, for the quintet state is slightly smaller, whereas for the highest spin is the largest one. The total charge on the O_2 ligand does not depend on the multiplicity and indicates its neutral character. In the singlet state the value of the O–O bond order is close to that observed in the neutral dioxygen molecule, whereas in the other states it is much lower. The decrease in the bond order is usually connected with the occupation of the antibonding orbitals and proceeds during the transformation of O_2 in to O_2^-.

Since in our case the charge on dioxygen is the same for all the states, such a transformation does not take place. The analysis of MO orbitals within the oxygen ligand indicates the rearrangement of electrons from two strong σ and one weaker π orbitals into one strong σ (for the single state) and two weaker π orbitals (for the triplet state), which explains the observed decrease in the bond order. The charges localized on the proximal histidine and on the porphyrin ring are similar for singlet, triplet and heptet states. They differ for the quintet state. The bond order analysis suggests a weak covalent bond between iron ion and dioxygen.

Table 4. Relative energies (0 value refers to the multiplicity with the lowest energy) and selected electronic properties for the different electronic states of the oxyheme (hemeO_2) system.

	singlet	triplet	quintet	heptet
Energy [kJ/mol]	215.55	69.31	46.73	0
Charges on atom or molecular fragments				
Fe	0.87 ($s^{0.262}p^{0.543}d^{6.320}$)	0.86 ($s^{0.284}p^{0.548}d^{6.310}$)	0.80 ($s^{0.321}p^{0.572}d^{6.309}$)	0.92 ($s^{0.303}p^{0.580}d^{6.198}$)
O_2	0.03	0.03	0.02	0.03
N(his)	–0.23	–0.23	–0.21	–0.24
proximal histidine	0.08	0.07	0.04	0.07
porphyrin ring	–2.95	–2.96	–2.84	–2.99
Bond orders				
Fe–O	0.20	0.17	0.16	0.15
O–O	1.97	1.48	1.48	1.48
Fe–N(his)	0.37	0.33	0.27	0.33

Oxidized oxyheme system: The oxidation of oxymyoglobin is modelled by removing one electron from the oxyheme system; the resulting hemeO_2^+ species is treated as a hypothetical intermediate in this model process. Three electronic states, namely doublet, quartet and sextet corresponding to 1, 3 and 5 unpaired electrons are considered for the oxidized oxyheme. The highest possible state (2S+1) = 8 is not discussed. Table 5 collects total energies and selected electronic properties for the different multiplicity states of the hemeO_2^+. Here, the total energy of the hemeO_2^+ depends on the multiplicity and, as it was in the case of the oxyheme, decreases with increasing the number of unpaired electrons. The least stable seems to be the doublet state, whose energy is equal to 283.29 kJ/mol higher than the energy of the quartet. The energy difference between the quartet and the sextet is about 60 kJ/mol.

Table 5. Relative energies (0 value refers to the multiplicity with the lowest energy) and selected electronic properties for the different electronic states of the oxidized oxyheme (hemeO_2^+) system.

	doublet	quartet	sextet
Energy [kJ/mol]	283.29	56.45	0
Charges on atom or molecular fragments			
Fe	0.89 ($s^{0.285}p^{0.530}d^{6.298}$)	0.85 ($s^{0.306}p^{0.535}d^{6.304}$)	0.88 ($s^{0.319}p^{0.602}d^{6.198}$)
O_2	0.03	0.03	0.03
N(his)	–0.19	–0.16	–0.15
proximal histidine	0.30	0.33	0.31
porphyrin ring	–2.22	–2.22	–2.22
Bond orders			
Fe–O	0.13	0.10	0.15
O–O	1.47	1.47	1.48
Fe–N(his)	0.36	0.26	0.26

There are at least two reasons to select the quartet as the ground state for the hemeO_2^+. First, the oxidation process does not change the charge on the iron atom (0.86 and 0.85 for the hemeO_2 and the hemeO_2^+, respectively), therefore the multiplicity of the iron should not be altered. Second, since the oxygen molecule is bound very weakly to the metheme, its spin state should be the same as in the isolated O_2, *i.e.* the triplet. Altogether, there should be three unpaired electrons in the system (two electrons on the oxygen and one on the iron). The experimental data suggest, that the natural aqua-metmyoglobin is a high-spin system [1,4]. There are no data for a hypothetical intermediate product the hemeO_2^+. Similar charge on Fe in the oxyheme and the oxidized oxyheme may suggest, that in the electron transfer process the heme iron does not undergo the oxidation. It mediates in removing an electron mainly from the porphyrin ring ($\Delta_{el} = 0.75$) and the proximal histidine ($\Delta_{el} = 0.25$). Charge on the oxygen ligand is independent of the system multiplicity and indicates its neutral, although, "excited" state. Charges on the proximal histidine and the porphyrin ring are similar for all states of different multiplicities.

The bond order analysis indicates a weak covalent bond between the heme iron and the oxygen molecule. This bond is the weakest in the case of the quartet state. The bond order for O–O (~1.5) is independent of the spin state. The Fe–N(his_p) bond is the strongest for the doublet state. Here, both the covalent contribution (seen directly from the bond order value) and the ionic one (indicated by the charge difference between Fe and N) are the biggest ones.

Aqua-metheme (metheme-H_2O): It is known that in natural metmyoglobin a water molecule occupies the sixth coordination site of the heme iron [19], whereas the

five-coordination heme compound of the iron(III) does not exist. In order to model the system realized in nature, the calculations for the six-coordinated heme complex, *i.e.* the aqua-metheme (a water molecule as the sixth ligand) are carried out. Similarly as for heme (Table 2), the quartet state is considered as the ground state. The geometry of aqua-metheme is optimized.

Table 6 compares the total energies and the selected electronic as well as geometrical parameters for two systems, the heme$^+$ and the metheme-H_2O, which can be assumed as models for the oxidized form of myoglobin. It is worth to emphasise a significant change in the charge distribution between the oxidized deoxyheme (heme$^+$) and the aqua-metheme (metheme-H_2O). First, an increase of the positive charge on the iron atom is observed (from 0.76 for the heme$^+$ to 0.85 for the metheme-H_2O). Moreover, the value of the charge on the heme iron atom in the aqua-metheme (0.85) is very similar to those obtained for the oxyheme (0.86) and the oxidized oxyheme (0.85), which suggests that iron is in the same oxidation state in all these cases.

Table 6. Selected geometrical as well as electronic properties for systems heme$^+$ and metheme-H_2O modelling the oxidized forms of myoglobin.

	heme$^+$	metheme–H_2O
Charges on atom or molecular fragments		
Fe	0.76	0.85
N(his)	–0.22	–0.15
histidine	–0.25	0.32
porphyrin ring	–1.51	–2.27
Distances [Å]		
Fe–O	–	2.24
Fe–N (his)	2.304	2.28
Bond orders		
Fe–O	–	0.26
Fe–N(his)	0.32	0.25

On passing from the heme$^+$ to the metheme-H_2O, one observes a decrease in the net charge on the nitrogen atom of the proximal hisidine (coordinated to the iron atom), (from –0.22 to –0.15) and a shift of 0.58e from the proximal histidine to the porphyrin ring. Additionally, both ionic and covalent contributions to the Fe–N(his_p) bond are smaller. The smaller ionic part derives from the smaller difference between Fe and N(his_p) charges. The smaller covalent contribution can be seen directly from Table 6 (0.25 against 0.32). Five- and six-coordinated porphyrin complexes differ significantly in the charge of porphyrin ring, which suggests that the porphyrin ring

participates directly in the oxidation process of heme. Addition of the water molecule does not cause a substantial change in the Fe–N(his_p) distance (2.30 Å and 2.28 Å for the $heme^+$ and the aqua-metheme, respectively).

Addition of the water molecule to the oxidized deoxyheme, which is schematically shown in Scheme 3 leads to the significant stabilization of the system.

$$heme^+ + H_2O \longrightarrow \text{metheme-}H_2O \qquad (3)$$

Large stabilization energy, that is equal to 588.64 [kJ/mol], suggests that the inclusion of the water molecule in the oxidized protein model (*via* its coordination to the iron in the sixth position) gives a better account of the possible natural process.

Oxyheme with the distal histidine: There are two histidine residues adjacent to the heme centre: a proximal one (coordinated to the heme iron) and a distal one (placed on the opposite side of the porphyrin plane and forming a hydrogen bond with the oxygen which is bound to the iron).

To model the $hemeO_2$–his_d the experimental geometry from the rentgenographic studies is taken as the starting point [18]. Then the positions of the iron, oxygen and hydrogen (forming the hydrogen bond) atoms are relaxed. The calculations are carried out for the triplet state, which is selected as the ground state in the case of the isolated oxyheme system.

Table 7 compares the charge distributions between the oxyheme and the oxyheme with the distal histidine. The introduction of the distal histidine causes only a very small change in the electronic structure of the oxyheme. The presence of the positively charged hydrogen atom of the distal histidine induces a slight shift of the electron density towards the terminal oxygen atom O(2). Also a small decrease of the charges on the iron and nitrogen (of the proximal histidine) atoms as well as on the porphyrin ring is observed.

The experimental data confirm the presence of the hydrogen bond between oxygen O(2) and the hydrogen from the distal histidine [52]. The results of calculations, *i.e.* the O–H bond distance (1.26 Å) as well as the bond order (0.19), clearly indicate the formation of a hydrogen bond rather than of a typical hydroxyl group.

The comparison of the O–O distances (1.11 Å and 1.12 Å) and bond orders (1.48 and 1.43) in the $hemeO_2$ and the $hemeO_2$–his_d reveals a slight increase of the distance and a decrease of the bond order, which may suggest a weakening of this bond. The increase of the Fe–O distance (from 2.28 Å to 2.36 Å) indicates a tendency to dissociation of the oxygen molecule from the protein model, however, the complete dissociation of the O_2 molecule from the $hemeO_2$–his_d is not observed, due to the stabilization of dioxygen *via* the hydrogen bond. Therefore, the [Fe--O_2--H(his_d)] structure can be proposed for the $hemeO_2$–his_d system.

The oxidation process: There are at least two reasons, why we have decided to study the myoglobin oxidation process for the first time by quantum chemistry. First, in the literature [20–30] one can find numerous contradictory statements on the description of the electronic structure of the protein active centre. Moreover, a new role

of hemoglobin and myoglobin in the intracellular reduction of metal ions is discovered [5–6]. Table 8 summarizes the electronic characteristics of the ground states of all the systems, which take part in the redox process. Among the presented compounds there are real reagents (heme, $hemeO_2$ and metheme-H_2O), as well as the species treated as hypothetical intermediate products in a redox reaction ($heme^+$ and $hemeO_2^+$).

Table 7. Selected electronic and geometrical properties for the oxyheme ($hemeO_2$) and the oxyheme with the distal histidine ($hemeO_2$–his_d).

	$hemeO_2$	$hemeO_2$–his_d
Charges on atom or molecular fragments		
Fe	0.86	0.80
O(1)	0.01	0.10
O(2)	0.02	–0.01
N(his)	–0.23	–0.20
proximal histidine	0.07	0.14
porphyrin ring	–2.96	–2.91
Distances [Å]		
Fe–O	2.28	2.36
O–O	1.11	1.12
Bond orders		
Fe–O	0.17	0.15
O–O	1.48	1.43

Table 8. Selected electronic and geometrical properties for the ground states of the studied heme species.

	heme	$heme^+$	metheme–H_2O	$hemeO_2$	$hemeO_2^+$
Charges on atom or molecular fragments					
Fe	0.76	0.76	0.85	0.86	0.85
O(1)	–	–	–	0.01	0.01
O(2)	–	–	–	0.02	0.02
N(his)	–0.22	–0.22	–0.15	–0.23	–0.16
histidine	–0.26	–0.25	0.32	0.07	0.33
porphyrin ring	–2.50	–1.51	–2.27	–2.96	–2.21

Table 8 (continuation)					
Distances [Å]					
Fe–O	–	–	2.24	2.28	2.43
O–O	–	–	–	1.11	1.12
Fe–N(his)	2.22	2.30	2.28	2.17	2.27
Fe–N(1)	2.08	2.03	1.94	1.94	1.94
Fe–N(2)	2.06	1.99	1.94	1.94	1.94
Fe–N(3)	2.17	2.09	1.96	1.95	1.95
Fe–N(4)	2.06	2.02	1.95	1.96	1.96
Bond orders					
Fe–O	–	–	0.26	0.17	0.10
O–O	–	–	–	1.48	1.47
Fe–N(his)	0.380	0.315	0.25	0.33	0.26

The oxidation process of the deoxyheme: Analysing the oxidation process of deoxymyoglobin (in our model heme) shown in Scheme 4, one has to remember that in reality this process is accompanied by the coordination of a water molecule and formation of a six-coordinated species. An isolated oxidation reaction, connected with the removal of one electron from the system, is a spontaneous process and is connected with the energetic effect of 368.10 kJ/mol. It leads, however, to the formation of a hypothetical five-coordinated heme complex of iron(III), that can be treated as an unstable intermediate only.

$$\text{heme-e}^- \xrightarrow{\Delta E = -368.10\ \text{kJ/mol}} \text{heme}^+ \qquad (4)$$

Scheme 5 analyses the same oxidation process, in which a water molecule is involved. Now, the energetic effect of the reaction is almost three times larger. The comparison of the electronic structure of the oxidized deoxyheme (heme^+) and the aqua-metheme (metheme-H_2O) leads to the conclusion, that heme^+ can be considered to be only an unstable intermediate product.

$$\begin{array}{l} \text{heme-e}^- \xrightarrow{\Delta E = -368.10\ \text{kJ/mol}} \text{heme}^+ \\ \qquad\qquad +H_2O \;\Big\downarrow \qquad \Delta E \cong -588.64\ \text{kJ/mol} \\ \qquad\qquad \text{metheme-}H_2O \end{array} \qquad (5)$$

The oxidation process of the oxyheme: The oxidation process of the oxyheme, realized by removing one electron from the system, leads to the species described by formula hemeO_2^+. Similarly, as it was in the case of the deoxyheme, the compound formed in this process can be treated only as an unstable product. It is highly possible, that this complex will easily dissociate the oxygen molecule. The analysis of the Fe–O bond length, as well as the bond order in the reduced and oxidized form of the oxyheme, allows us to conclude the dissociation of dioxygen. The weakening of the Fe–O bond results from an increase in the Fe–O bond distance (from 2.28 Å to 2.43 Å) and a decrease in the bond order (from 0.17 to 0.10) for the oxyheme and the oxidized oxyheme, respectively (see Tables 4 and 5). The obtained values do not indicate a total cleavage in the Fe–O bond. It is worth pointing out, that the oxidation reaction is an exothermic one, even though the oxidized oxyheme, can be treated as an unstable intermediate only.

Studying the oxyheme oxidation, one should remember that the final product is the aqua-metheme, as it is in the case of the deoxyheme. This process consists of few steps and its energetic effect follows not only from the removal of one electron from the system, but also from the dissociation of the dioxygen molecule and addition of the water molecule. Therefore, two pathways should be examined for the oxidation process of the oxyheme:

– the dissociation of the oxygen molecule and the addition of the water molecule being parallel processes, as shown in Scheme 6.

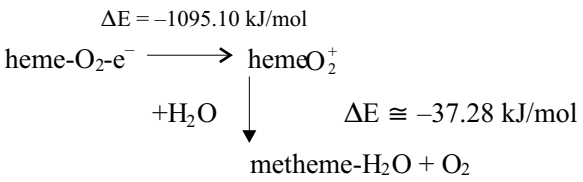

(6)

– the dissociation of O_2 proceeding prior to the addition of the water molecule as shown in Scheme 7.

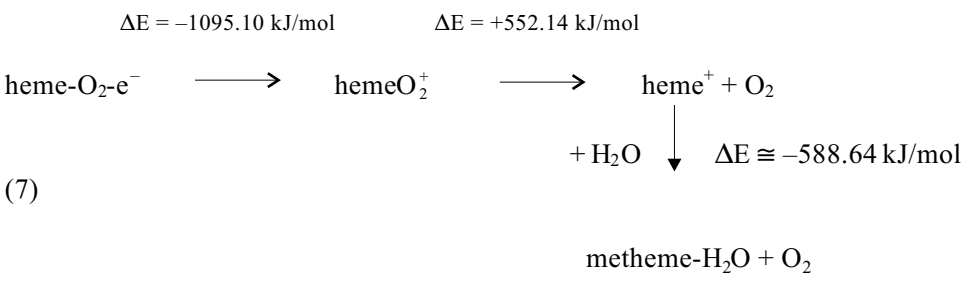

(7)

In both cases, the energetic effect is about 1100 kJ/mol. As one can see from the comparison of the total energies of the intermediates, each of the elementary steps in the first reaction pathway proceeds spontaneously. In the second route (Scheme 7) already the elementary step from the hemeO_2^+ into the heme$^+ + O_2$ costs 0.21 a.u. (~550 kJ/mol) and will not occur spontaneously. This allows us to suggest the first reaction pathway as the preferable one.

One should stress, that the optimized electronic and geometric structures of the deoxy- and the oxyheme with coordinated proximal histidine species, as well as of their one-electron oxidized forms are obtained by use of semiempirical quantum chemistry treatment. Although various theoretical approaches and different models of the active centre of oxygen carrying hemoproteins have been applied to describe the nature of the Fe–O_2 bonding, our work focused on the real oxyheme (IX protoporphyrin-Fe–O_2) with coordinated histidine.

The analysis of the iron atomic charge for all the studied systems shows, that iron has the lowest charge in the deoxyheme (Fe(II)). This charge increases during the oxidation process. For the other moieties (hemeO_2, hemeO_2^+ and metheme-H_2O), the charge on Fe atom is similar and bigger than in the deoxyheme. Therefore, one can conclude that in the oxyheme species iron exists as Fe(III).

The introduction of the distal histidine causes only a slight weakening of the Fe–O_2 bond in the case of the oxyheme species. At the same time, it points out to the shift of the negative charge towards the second atom of the O_2 ligand and a possibility of the formation of the hydrogen bond between the oxygen ligand and the hydrogen atom from the distal histidine residue.

This work presents the first investigation of the electron transfer process for the model of myoglobin active centre, by means of quantum chemical approach. The analysis of the energetics indicates, that both deoxy- and oxyheme species can undergo spontaneous oxidation processes. In the case of the deoxyheme, addition of the water molecule to the free coordination site of the Fe(III) in the heme$^+$, not only stabilizes the system, but also induces such changes in the electronic structure that it comes closer to that suggested in the Weiss' model. For the oxyheme system, we have investigated two reaction pathways for the overall oxidation process. The results of our calculations indicate that the pathway, in which the step of substitution of dioxygen by the water molecule proceeds according to the associative or inter-change associative mechanism, is more favourable than the one, which proceeds according to the dissociative mechanism.

It is generally known, that semiempirical quantum chemical methods gain speed in computation by neglecting many of the integrals, following from the first principles or by approximating them either to experimental data or to the *ab initio* results. Therefore, in many cases semiempirical methods, that are well parameterized, give results of the same accuracy as *ab initio* treatment in sense of the agreement with experiment. The ZINDO method, that is used in the presented calculations, is parameterized for spectroscopic properties of molecules and complexes with transition metals. The method is capable to generate reliable ground state geometries, transition

state barriers, as well as to reproduce UV/Visible spectra of molecules. However, as any of the semiempirical methods, it is not free of the typical errors connected with for example lack of the diffuse functions (as a result it cannot well reproduce exited states that are primarily Rydberg in nature). In addition, since it does not have any treatment beyond the SCF level, the energy of high laying states is not in good accordance with experimental values. We are aware of that the detailed description of the excited states of transition metal complexes requires the CI or multiconfiguration SCF (MC SCF) treatments, but also of the fact that all these approaches are time consuming, especially for large systems like myoglobin active center.

The details of the iron–O_2 bonding is another point, in which more profound treatment could be helpful. The understanding of the binding of the molecular oxygen to the metallic center, which seems to be essential in explaining the metal – ligand charge transfers (an enrichment in electrons of π^* O_2 orbitals without net charge transfer onto oxygen atoms) induced by the complex formation would required at least MC SCF methods.

Keeping the restriction of ZINDO method in mind, we are still convinced that the present studies are fruitful and may provide same insight into the redox processes, that may occur in the myoglobin active center.

Acknowledgments

The authors gratefully acknowledge financial support from the Polish State Committee for Scientific Research (KBN), grants No 0202/T09/97/13 and 071/T09A/115/15 (E.I. and G.S.)

REFERENCES

1. Bertini I., Gray H.B., Lippard S.J. and Valentine J.S., Bioinorganic Chemistry, University Science Books, Mill Valley, California (1994).
2. Lippard S.J. and Berg J.M., Principles of Bioinorganic Chemistry. University Science Books, Mill Valley, California (1994).
3. Heremans K., In van Eldik R., Jonas J., Reidel J. (eds), High Pressure Chemistry and Biochemistry. Publishing Company, Dordrecht, Holland (1987).
4. Spiro T.G., In Lever A.B.P., Gray H.B. (eds), Iron porhyrins. Addison-Weslay, Part II, p. 89 (1983).
5. Hegetschweiler K., Saltman P., Dalvit C. and Wright P.E., *Biochim. Biophys. Acta*, **912**, 384 (1987).
6. Eguchi L.A. and Saltman P., *Inorg. Chem*., **26**, 3665 (1987).
7. Egyed A. and Saltman P., *Biol. Trace Element. Res*., **6**, 357 (1984).
8. Bothwell T.H., Charlton R.W., Cook J.D. and Finch C.A., in: Iron Methabolism in Man. Blackwell Scientific, London (1979).
9. Egyed A., May A. and Jacobs A., *Biochim. Biophys. Acta*, **629**, 391 (1980).
10. Antonini E., Bronori M. and Wyman J., *Biochem*., **4**, 545 (1965).
11. Zhang B-J., Andrwe C.R., Tomkinson N.P. and Sykes A.G., *Biochim. Biophys. Acta*, **1102**, 245 (1992).
12. Ilkowska E., van Eldik R. and Stochel G., *J. Biol. Inorg. Chem*., **2**, 603 (1997).
13. Kawanishi S. and Caughey W.S., *J. Biol. Chem*., **260**, 4622 (1985).
14. Kruszyna H., Kruszyna R., Rochelle L.G., Smith R.P. and Wilcox D.E., *Biochem. Pharmacol*., **46**, 95 (1993).
15. Butler A.R. and Glidewell Ch., *Chem. Soc. Rev.*, **16**, 361 (1987).
16. Ilkowska E., Lewiński K., van Eldik R. and Stochel G., *J. Biol. Inorg. Chem*., **4**, 302 (1999).

17. Takano T., *J. Mol. Biol*., **110**, 569 (1977).
18. Philips S.E.V., *J. Mol. Biol*., **142**, 531 (1980).
19. Takano T., *J. Mol. Biol*., **110**, 537 (1977).
20. Pauling L., *Nature*, **203**, 182 (1964).
21. Weiss J.J., *Nature*, **202**, 83 (1964).
22. Newton J.E. and Hall M.B., *Inorg. Chem*., **23**, 4627 (1984).
23. Dedieu C., Rohmer M.M. and Veillard A., *J. Am. Chem. Soc*., **98**, 5789 (1976).
24. Dedieu C., Rohmer M.M., Veillard H. and Veillard A., *Nouv. J. Chem*., **3**, 653 (1976).
25. Yamamoto S. and Kawanishi H., *Chem. Phys. Lett*., **161**, 85 (1989).
26. Yamamoto S. and Kawanishi H., *Chem. Phys. Lett*., **205**, 306 (1993).
27. Nozawa T., Hatano M., Nagashima K., Obara S. and Kashiwagi H., *Bull. Chem. Soc. Jpn*., **56**, 1721 (1983).
28. Bertan J., Ruiz-López M.F. and Rinaldi D., *J. Mol. Struct.(Theochem)*, **232**, 337 (1991).
29. Rovina A., Kunc K., Hutter J., Ballone P. and Parrinello M., *Int. J. Quant. Chem*., **69**, 31 (1998).
30. Bytheway I. and Hall M.B., *Chem. Rev*., **94**, 639 (1994).
31. Ridley J. and Zerner M.C., *Theoret. Chim. Acta*, **32**, 111 (1973).
32. Bacon A.D. and Zerner M.C., *Theoret. Chim. Acta*, **53**, 21 (1979).
33. Zerner M.C., Loew G.H., Kirchner R.F. and Mueller U.T., *J. Am. Chem. Soc*., **102**, 589 (1980).
34. Edwards W.D. and Zerner M.C., *Theoret. Chim. Acta*, **72**, 347 (1987).
35. Slater J.C., *Phys. Rev*., **36**, 57 (1930).
36. Head J.D. and Zerner M.C., *Chem. Phys. Lett*., **122**, 264 (1985).
37. Edwards W.D., Weiner B. and Zerner M.C., *J. Am. Chem. Soc*., **108**, 2196 (1986).
38. Wasielewska E., Witko M., Stochel G. and Stasicka Z., *Chemistry – A European Journal*, **3**, 609 (1997).
39. Edwards W.D., Weiner B. and Zerner M.C., *J. Phys. Chem*., **92**, 6188 (1988).
40. Anderson W.P., Edwards W.D. and Zerner M.C., *Inorg. Chem*., **25**, 2728 (1986).
41. Loew G.H., Herman Z.S. and Zerner M.C., *Int. J. Quantum Chem*., **33**, 177 (1988).
42. Anderson W.P., Edwards W.D., Zerner M.C. and Canuto S., *Chem. Phys. Lett*., **88**, 185 (1982).
43. Stavrev K.K. and Zerner M.C., *Chem. Europ. J*., **2**, 34 (1996).
44. Mulliken R.S., *J. Chem. Phys*., **23**, 1833, 1841, 2343, 2388 (1955).
45. Mayer I., *Chem. Phys. Lett*., **97**, 270 (1983).
46. Mayer I., *J. Mol. Struct.(Theochem)*, **81**, 14 (1987).
47. Kashiwagi H., in: Nagata *et al*. (eds), Biomolecules. Japan Sci. Soc. Press, Tokyo, p. 31 (1985).
48. Rohmer M.M., in: A. Veillard (ed), Quantum Chemistry: The Challenge of Transition Metals and Coordination Chemistry, D. Reidel Publishing Co Dordrecht, Holland, p. 377 (1986).
49. Lang G. and Marshall W., *J. Mol. Biol*., **18**, 385 (1966).
50. Dedieu C., Rohmer M.M. and Veillard A., in: Pullman B., Goldblum N. (eds), Metal-Ligand Interactions in Organic Chemistry and Biochemistry. Part 2, D. Reidler Publishing Co., Dordrecht, Holland, pp. 101 (1977).
51. Smith T.D. and Pilbrow J.R., *Coord. Chem. Rev*., **39**, 295 (1981).
52. Norvell J.C., Nunes A.C. and Schoenborn B.P., *Science*, **190**, 568 (1975).